JOURNAL OF GEOPHYSICAL RESEARCH, VOL. 105, NO. C7, PAGES 16,783–16,801, JULY 15, 2000

Mixed layer depth variability and barrier layer formation over the North Pacific Ocean

A. Birol Kara

Advanced Systems Group, Sverdrup Technology, Inc., Stennis Space Center, Mississippi

Peter A. Rochford and Harley E. Hurlburt

Oceanography Division, Naval Research Laboratory, Stennis Space Center, Mississippi

Abstract. Seasonal variability in the isothermal and isopycnal surface mixed layers of the North Pacific Ocean is examined using the Naval Research Laboratory Ocean Mixed Layer Depth (NMLD) Climatology. A comparison with observations from 11 ocean weather stations in the northeast Pacific Ocean is performed that validates the NMLD climatology in this region. The general features of the isothermal layer depth (ILD) and mixed layer depth (MLD) obtained from these mixed layers are explained with wind stress, surface net heat flux, and freshwater flux climatologies, given guidance from a mixed layer model. Departures from a surface-forced interpretation of turbulent mixing are found near the Kuroshio, where horizontal heat transport is important. The much deeper ILD in the northeast Pacific in winter and spring relative to the MLD reveals a 50 m "barrier layer" between the bottom of the MLD and the top of the thermocline. A detailed analysis shows this barrier layer extends over most of the North Pacific subpolar gyre. It forms when the seasonal thermocline is deepened in winter by surface cooling, such that salinity stratification due to evaporation minus precipitation less than zero ($E - P < 0$) becomes important in the formation of the MLD. A shallower halocline forms over the subpolar gyre than in other regions of the North Pacific because of precipitation dominating over evaporation in the annual mean. A mechanism for maintaining the shallow halocline is provided by upward vertical motion driven by positive wind stress curl in the presence of diapycnal mixing. Numerical models show this as part of a shallow meridional overturning cell.

1. Introduction

Studies have shown there are regions in the world ocean where the top of the thermocline is deeper than the pycnocline with large differences in their depths [e.g., *Lindstrom et al.,* 1987; *Lukas and Lindstrom,* 1991; *Sprintall and Tomczak,* 1992]. In all these studies an isothermal layer depth (ILD) and mixed layer depth (MLD) were defined for the isothermal and isopycnal surface layers, respectively, to characterize these differences. This difference between the ILD and MLD has been described as a barrier layer [*Lukas and Lindstrom,* 1991; *You,* 1995] and has been an active subject of research in the past few years. Most of this focus has been in the equatorial Pacific Ocean because of the consequences the barrier layer can have upon ocean heat budgets [*Swenson and Hansen,* 1999], sea surface temperature (SST), and thereby heat exchange with the atmosphere [e.g., *Enfield,* 1986; *Chen et al.,* 1994]. The presence of a barrier layer reduces entrainment cooling in the mixed layer, except during strong wind events [*Niiler and Stevenson,* 1982; *Meyers et al.,* 1986]. Effort has also been directed toward understanding the formation of the barrier layers [*Vialard and Delecluse,* 1998; *You,* 1998] and their frequency of occurrence with SST variability [*Ando and McPhaden,* 1997].

While much attention has been devoted to the barrier layer of the equatorial Pacific, little attention has been given to the barrier layer that is noted to form in the North Pacific [*Monterey and Levitus,* 1997; *Sprintall and Roemmich,* 1999]. In contrast to the 20–40 m thick barrier layers that occur in the equatorial region, much thicker barrier layers of up to 100 m form during winter in the 45°–60°N latitudes and then disappear during summer. The formation of this layer is clearly a characteristic of the seasonal variability in the ILD and MLD in the North Pacific. The influence of salinity stratification included in the MLD is evidently important for its formation [e.g., *Miller,* 1976; *Piola and Gordon,* 1984; *Sprintall and Tomczak,* 1992]. Yet how does salinity stratification play a role?

Paper number 2000JC900071.
0148-0227/00/2000JC900071$09.00

Studies of the equatorial Pacific have revealed that surface freshwater fluxes (i.e., heavy rainfall with the effect of horizontal advection) and strong wind bursts are responsible for the formation of the equatorial barrier layer [*Ando and McPhaden,* 1997; *Vialard and Delecluse,* 1998; *Godfrey and Lindstrom,* 1989]. As described by *Anderson et al.* [1996], this barrier layer formation occurs because strong wind bursts deepen the surface mixed layer to the top of the thermocline and precipitation and surface heating increase the surface buoyancy, forming a relatively warm and fresh thin surface mixed layer. Are similar or different processes responsible for the North Pacific barrier layer at midlatitudes? Direct surface ventilation of the upper layers of the North Pacific is known to be quite shallow because of the relatively low density of the surface waters in winter and the presence of saline deep waters [e.g., *Yuan and Talley,* 1992]. *Tsuchiya* [1982] showed that the shallow salinity minima of the North Pacific can be related to the subduction (possibly when ILD < MLD) of surface waters. The formation of the North Pacific barrier layer can be answered by understanding the reasons for the seasonal variability in the ILD and MLD. Henceforth we shall use LD to denote ILD and MLD whenever the latter can be commonly referred to in the given context.

A basin-scale study has been done on the seasonal changes in surface LD for the Pacific Ocean [*Bathen,* 1972], using an ILD definition applied to a monthly mean climatology constructed from observations. In that study the depth of mixing is defined using a temperature definition with a prescribed temperature gradient of 0.02 °C m^{-1} because at the time the salinity observations needed were much less common for large regions of the world's oceans. With the present availability of higher-resolution global ocean climatologies for temperature [*Levitus et al.,* 1994], salinity [*Levitus and Boyer,* 1994], wind stress, heat flux, and freshwater flux [e.g., *da Silva et al.,* 1994], not only is investigating seasonal variability of isothermal and isopycnal mixed layers possible, but so is interpreting them in terms of surface-forced turbulent mixing [*Price et al.,* 1986; *Gordon and Corry,* 1991], which can provide insight into the physical processes that are responsible for the formation of the winter barrier layer in the North Pacific. Given the known sensitivity of the LD to the criteria used to define them [*Kara et al.,* this issue], be it a property gradient definition or a property change definition, appropriate care must be taken to apply an optimal definition.

The major circulation systems in the North Pacific [e.g., *Talley,* 1993; *Hurlburt et al.,* 1996; *Shriver and Hurlburt,* 1997] are found to influence the seasonal variability in LD in certain regions of the basin [*Qiu and Joyce,* 1995]. The surface circulation in the Pacific consists of the cyclonic subpolar gyre in the north, the anticyclonic North Pacific subtropical gyre, and the north Equatorial Counter current near the equator [e.g., *Talley,* 1993]. *Roden* [1979] explained that a correlation exists between the positions of the North Pacific Current and the MLD variations. *Monterey and Levitus* [1997] noted a few small regions in the North Pacific where ILD is shallower than MLD, occurring inside the subtropical gyres during March and April. Differential radiative heating can sharpen or weaken existing temperature fronts in the North Pacific because radiative heat fluxes are effective in changing the temperature of the upper layer and in altering the hydrostatic stability [e.g., *Roden,* 1980; *Dinniman and Rienecker,* 1999]. Horizontal heat transport by advection and diffusion can alter local heat balances in the North Pacific [*Gent,* 1991; *Qiu and Kelly,* 1993], which in turn, diminish or enhance the amount of turbulent mixing. Thus we also investigate if the ILD and MLD depart in the North Pacific from expectations derived from the surface forcing as given by heat, freshwater fluxes, and wind stress, such as in the region of the Kuroshio.

This paper is organized in the following manner. In section 2 we briefly describe the ILD and MLD climatologies used for this study. Subsequently, in section 3 we analyze the latitude dependence of the ILD and MLD over the entire North Pacific Ocean to validate the use of *World Ocean Atlas 1994* data [*Levitus et al.* 1994; *Levitus and Boyer,* 1994] (hereinafter referred to as Levitus data) to infer such ILD and MLD. In section 4 we investigate the seasonal dependence of the ILD and MLD and explain it in terms of turbulent mixing. In section 5 we specifically examine the subarctic barrier layer. In section 6 we present conclusions. This paper serves as a first application of the NMLD climatologies and introduces them for use by the research community.

2. ILD and MLD Climatologies

Explaining why the midlatitude barrier layer occurs for the region (0–65°N, 120°E–120°W) requires using LD climatologies that encompass the North Pacific Ocean. While ILD climatologies have been created in the past for individual ocean basins [e.g., *Bathen,* 1972; *Lamb,* 1984; *Rao et al.,* 1989], most climatologies used recently for studies requiring LD [e.g., *Ohlman et al.,* 1996; *Obata et al.,* 1996] have been constructed using temperature and salinity climatologies in the *World Ocean Atlas 1994* [*Levitus et al.,* 1994; *Levitus and Boyer,* 1994]. Here we use the Naval Research Laboratory Ocean ILD and MLD (NMLD) climatologies that are constructed from the monthly temperature and salinity climatologies of the Levitus data.

The methodology for inferring the ILD and MLD is fully described elsewhere [*Kara et al.,* this issue]. The ILD (MLD) can be summarized in its simplest form as being the depth at the base of an isothermal (isopycnal) layer, where the temperature (density) has changed by a fixed amount of ΔT ($\Delta\sigma_t = \sigma_t(T + \Delta T, S, P) - \sigma_t(T, S, P)$, where $P = 0$) from the temperature (density) at a reference depth of 10 m. See *Kara et al.* [this

Table 1a. Percentage of Barrier Layer Thicknesses

	Feb., %	May, %	Aug., %	Nov., %
$\Delta h <$ -60 m	0.2	0.0	0.0	0.0
-60 $\leq \Delta h <$ -50 m	0.3	0.0	0.0	0.0
-50 $\leq \Delta h <$ -40 m	0.8	0.1	0.0	0.0
-40 $\leq \Delta h <$ -30 m	2.5	0.2	0.0	0.0
-30 $\leq \Delta h <$ -20 m	3.0	0.2	0.0	0.0
-20 $\leq \Delta h <$ -10 m	6.4	0.1	0.1	0.4
-10 $\leq \Delta h <$ 0 m	11.3	13.0	14.4	15.1
0 $\leq \Delta h <$ 10 m	33.9	52.2	76.8	56.7
10 $\leq \Delta h <$ 20 m	15.0	20.0	7.1	18.5
20 $\leq \Delta h <$ 30 m	5.1	6.4	1.3	5.3
30 $\leq \Delta h <$ 40 m	4.2	2.4	0.3	1.7
40 $\leq \Delta h <$ 50 m	3.3	1.4	0.0	0.8
50 $\leq \Delta h <$ 60 m	2.9	1.1	0.0	0.4
60 $\leq \Delta h$	11.1	2.9	0.0	1.1

Percentage of barrier layer thicknesses ($\Delta h = h_L(T) - h_L(\sigma_t)$) for 10 m class intervals over the entire North Pacific Ocean. The results are shown for each season. The percentage probability of the absolute barrier layer thicknesses ($|\Delta h|$) is also given for each season.

issue] for a more precise and detailed definition. Note that both the ILD and MLD are defined by a ΔT criterion, with a $\Delta\sigma_t$ derived from a ΔT in the case of MLD. This approach has the advantage of allowing ILD and MLD comparisons, where the $\Delta\sigma_t$ for a MLD is related to the same ΔT used in defining an ILD while allowing either ΔT or $\Delta\sigma_t$ to determine the depth of mixing as appropriate. However, the latter does give a bias to MLD relative to ILD (typically MLD < ILD) when both temperature and salinity participate in the determination of MLD, and this bias slightly increases as the ΔT criterion increases. The bias is shallow (deep) when salinity increases (decreases) with depth above the ILD.

In the rest of the paper we implement our optimal definition of ΔT=0.8°C. Other studies have shown that local vertical gradient definitions for the ILD and MLD yield basically the same results as using a bulk difference in the temperature and density, respectively [*Ando and McPhaden,* 1997]. In the rest of the paper we also limit our consideration to the months of February, May, August, and November, which represent winter, spring, summer, and fall, respectively.

3. Latitudinal Variability of ILD and MLD

To gain initial insight into the formation of the barrier layer, we undertake here a study of the latitude dependence of the ILD and MLD over the North Pacific. This reduces the amount of information to examine and provides a simple first picture of the seasonal variability in LD. Analyzing the differences between the ILD and MLD values over the North Pacific with respect to latitude is a natural choice because like most oceanographic quantities, these LD may vary strongly with latitude [e.g., *Lamb,* 1984; *Teague et al.,* 1990]. We apply a ΔT=0.8°C criterion because this was found to yield an optimal ILD and MLD from an earlier study [*Kara et al.,* this issue]. We elected to calculate the mean and standard deviation layer depth for each 5° latitude belt using each 1° × 1° latitude-longitude box in that belt (Figure 1). In February the mean ILD and MLD are almost the same for each latitude belt below 40°N, with the same being true for the standard deviation. At latitudes above 40°N the means and standard deviations are significantly larger for the ILD ($h_L(T)$) relative to those for the MLD [$h_L(\sigma_t)$]. The results in Figure 1 confirm that substituting the ILD for the MLD north of 40°N will result in large errors for the MLD over much of the year. To a lesser extent this is also the case at low latitudes. The most consistent mean and standard deviation values between ILD and MLD are seen in August as they are relatively large in regions close to the equator and generally decrease with increasing latitude.

The ILDs are usually deeper than the MLDs over the North Pacific Ocean (Tables 1a and 1b), indicating the presence of barrier layers over large regions of the basin. The bias inherent in our method of definition, which is usually toward a shallower MLD, does not account for differences between the ILD and MLD $>\approx$ 20 m. For example, 20 m differences in mean val-

Table 1b. Percentage Probability of Absolute Barrier Layer Thickness ($|\Delta h|$)

	Feb., %	May, %	Aug., %	Nov., %
$\|\Delta h\| \geq$ 10 m	54.8	34.8	8.8	28.2
$\|\Delta h\| \geq$ 20 m	33.4	14.7	1.6	9.3
$\|\Delta h\| \geq$ 30 m	25.2	8.1	0.3	4.0
$\|\Delta h\| \geq$ 40 m	18.6	5.5	0.0	2.3
$\|\Delta h\| \geq$ 50 m	14.5	4.0	0.0	1.5
$\|\Delta h\| \geq$ 60 m	11.3	2.9	0.0	1.1

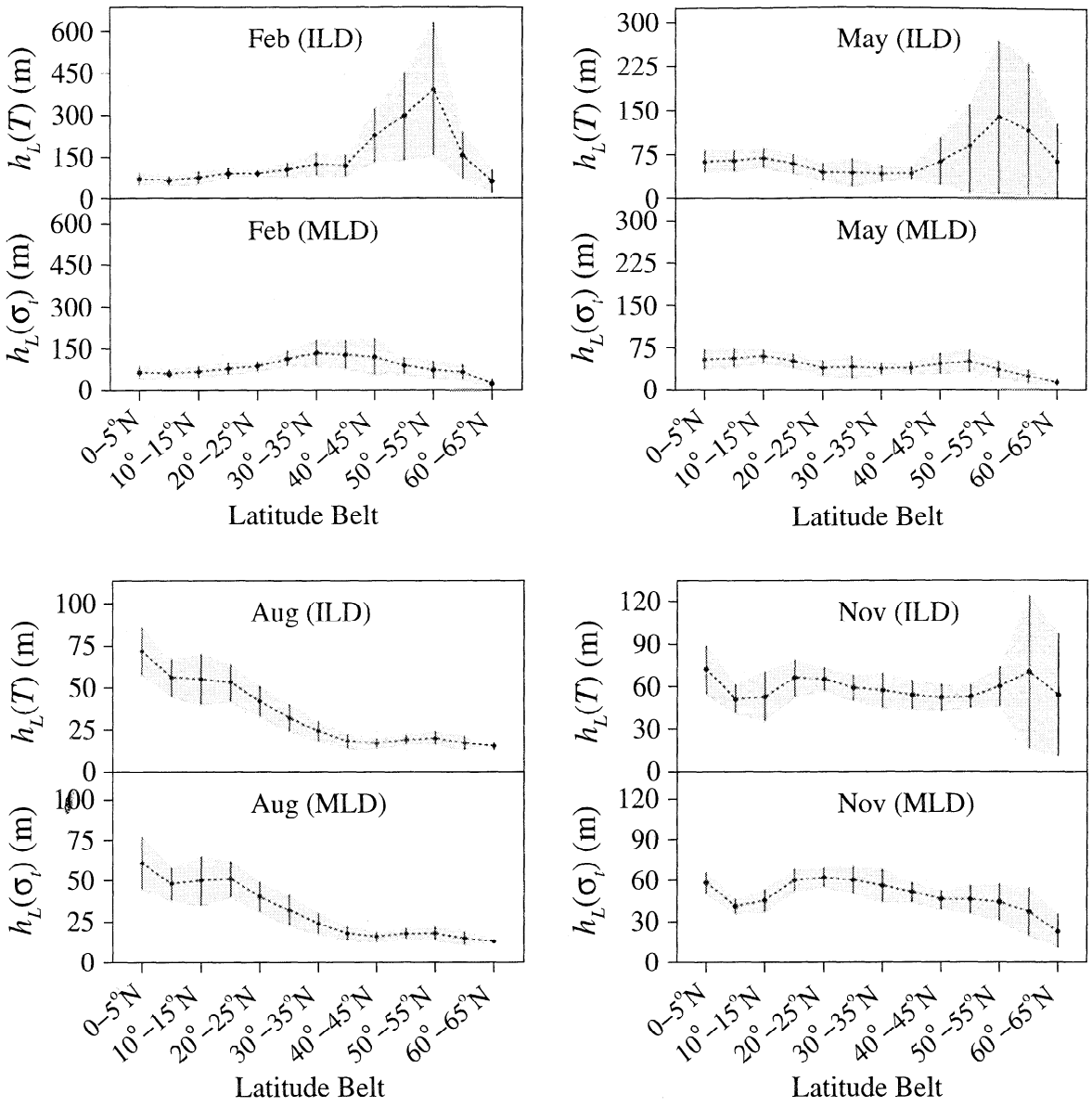

Figure 1. Mean ILD and MLD values for 5° latitude belts in the North Pacific Ocean for February, May, August, and November. Each dot denotes the mean for a given latitude belt, and the ranges shown (solid segments) are for 2 standard deviations from the mean. Note that vertical scaling is different for each season and that the x axis is labeled for every other 5° latitude belt.

ues near the equator in Figure 1 are known to result from physical processes as discussed earlier. We define the barrier layer thickness as $\Delta h = h_L(T) - h_L(\sigma_t)$ and note that it can have negative values as indicated by *Ando and McPhaden* [1997]. While the barrier layer thicknesses in each season are generally small (between 0 and 10 m), the number of cases for this class interval (i.e., $0 \leq \Delta h < 10$ m) becomes less than half of the total in February (33.9%). Note that barrier layers > 60 m thick occur over 11.1% of the basin latitude-longitude boxes in February. When the barrier layers are examined using absolute values of differences ($|\Delta h|$), use of an ILD for the MLD can evidently result in large differences in winter, and one must be cautious in making such an association. For example, a barrier layer thickness > 40 m occurs over 19.0% of the North Pacific in February but covers only 5.5% of the basin in spring and 2.3% in fall. In summer an ILD can be used for a MLD because only 1.6% (0.3%) of the basin has barrier layer values > 20 m (> 30 m).

To investigate the statistical nature of the barrier layer thickness (i.e., $\Delta h = h_L(T) - h_L(\sigma_t)$), a normalized rms (nrms) difference and rms difference are used:

$$\text{rms} = \sqrt{\frac{1}{n}\sum[h_L(T) - h_L(\sigma_t)]^2} \qquad (1)$$

$$\text{nrms} = \sqrt{\frac{1}{n}\sum\left[\frac{h_L(T) - h_L(\sigma_t)}{h_L(\sigma_t)}\right]^2}, \qquad (2)$$

where n denotes the number of cases. The LD is normalized (i.e, nrms) to eliminate the effects of seasonal changes, such as the much larger winter MLD relative to the summer MLD. The nrms and rms values are calculated for each season in 5° latitude belts starting from the equator (0–5°N) and proceeding northward (Table 2). Each latitude belt contains a different number of 1° × 1° latitude-longitude boxes, so the number of LD (n) in each latitude belt varies.

Obviously large nrms and rms barrier layer thickness values predominate for latitudes > 40°N, especially for February, May, and November (Table 2). In fact, the largest nrms values are seen at high midlatitudes (north of 45°N). Note that all 11 Ocean Weather Stations, which were used for analyses in *Kara et al.* [this issue], are located in the 45°–50°N latitude belt and therefore capture the relatively large MLD variability in the North Pacific Ocean. For August, barrier layer thicknesses are relatively small in comparison to those in other months and have the smallest rms values for latitude bands north of 10°N. The largest rms values are at lower latitudes. In general, for the nonsummer months a thin barrier layer at low latitudes exists but a much greater barrier layer thickness exists generally north of ≈ 40°N. Given that barrier layer thicknesses in the western equatorial Pacific inferred from direct observations have been found to be much thinner (5 m) than the climatological estimates of 25 m [*Anderson et al.*, 1996], we set 20 m as a safe limit for the significance of the mean barrier layer thickness and assume the mean ILD and MLD to be coincident whenever $\Delta h \leq 20$ m. Note that the nrms values given here were calculated across the latitude band, and therefore at low latitudes the larger values in the western equatorial Pacific are balanced by the negligible barrier layer thicknesses in the eastern half of the basin. This is confirmed by the barrier layer thicknesses in the 0–5° latitude band of the western equatorial Pacific (120°–180°E) having larger nrms and rms values relative to the eastern region (180°–240°E), as given in Table 2.

4. MLD Over the North Pacific

The preceding statistical analyses have shown that substantial seasonal variability exists in barrier layer thickness over the North Pacific, with the largest nrms occuring in the 45°–60°N latitude band. This thick barrier layer has been previously noted to occur during winter [e.g., *Monterey and Levitus*, 1997]. Since salinity stratification is clearly responsible for its occurrence, we will explain why salinity stratification becomes important for barrier layer formation in nonsummer months. This can be determined by investigating the physical origin of the ILD and MLD seasonal variability and how it leads to the seasonal formation of the barrier layer in the North Pacific Ocean. For this purpose the ILD and MLD are obtained using the optimal definition of ΔT=0.8°C. We again limit consideration to the middle month of each season.

4.1. Basin-Scale Variation

In February the ILD and MLD are found to be in general agreement at low latitudes, i.e., south of 30°N, with depths ranging from 50 to 125 m (Plate 1). Their uniformity and large-scale variations reflect the averaging associated with using a monthly mean climatology.

Table 2. The rms and nrms Barrier Layer Thickness over the North Pacific Ocean

Latitude		February		May		August		November	
Belt	n	nrms	rms, m	nrms	rms, m	nrms	rms, m	nrms	rms, m
east 0–5°N	304	0.01	4	0.09	5	0.13	8	0.28	15
west 0–5°N	300	0.22	12	0.36	15	0.38	19	0.48	18
0–5°N	604	0.17	9	0.26	11	0.37[a]	19	0.39	17
5°–10°N	598	0.11	7	0.19	10	0.24	14	0.29	9
10°–15°N	594	0.15	10	0.21	13	0.18	9	0.24	10
15°–20°N	598	0.27	16	0.21	11	0.10	6	0.15	8
20°–25°N	600	0.25	16	0.19	9	0.10	4	0.08	5
25°–30°N	600	0.14	16	0.17	8	0.08	3	0.07	4
30°–35°N	578	0.14	20	0.19	8	0.07	3	0.12	6
35°–40°N	541	0.23	24	0.30	7	0.05	2	0.13	6
40°–45°N	506	1.37	92	0.54	43	0.07	1	0.24	9
45°–50°N	474	1.41	133	1.46	88	0.08	1	0.35	10
50°–55°N	433	1.89[a]	184	1.68[a]	98	0.10	2	0.85	22
55°–60°N	347	1.62	161	1.65	107	0.12	2	1.42[a]	62
60°–65°N	83	1.29	109	1.08	81	0.18	2	1.27	92

Note that the nrms values are unitless, while the rms values are in meters. The analyses are performed for each month separately. The total number of mixed layer depth values (n) obtained from the sum of 1° × 1° latitude-longitude boxes for each latitude belt is also given. For the 0–5°N latitude belt, values are given separately for the east and west equatorial Pacific Ocean (east 0 − 5°N and west 0 − 5°N).

[a] The largest nrms barrier layer thickness value for the given month.

At midlatitudes, mean depths of more than 250 m occur for $h_L(T)$ in the 40°–55°N latitude band, while $h_L(\sigma_t)$ reaches maximum depths of 175–225 m in the western mid-Pacific east of Japan. The deep winter structure of the ILD is in general agreement with that reported by *Bathen* [1972] south of 40°N. He found the annual amplitude to be almost the same across the middle and low latitudes. The deeper ILD observed in the NMLD climatology at higher latitudes is not observed by *Bathen* [1972] because of the methodology used in his work. He used a combination of one subjective and two statistical methods to determine the ILD, and the thermal gradient criterion of one of these statistical methods yields an ILD that lies at a shallower depth beneath the pycnocline. Hence the subarctic layer depth reported by *Bathen* [1972] lies intermediate between our ILD and MLD. The much deeper ILD than MLD obtained in our work results in a significant barrier layer of more than 50 m for the subarctic (Plate 1).

The 10-30 m larger MLD than ILD in the western mid-Pacific east of Japan occurs because of the westward penetration of colder, fresher water from the central Pacific. Examination of the monthly Levitus temperature and salinity along 35°N from 145°E to 170°W reveals that this penetration brings an influx of water with a weak thermocline and an almost homogeneous halocline down to 225 m. The continued presence of the thermocline is what results in a shallower ILD than MLD. The westward penetration of this water likely occurs because of a relaxation in the strength of the Kuroshio during winter.

Elsewhere, the ILD and MLD rarely differ by more than 30 m. In some regions in the western equatorial Pacific the barrier layer is 30 m or greater. The burden of evidence indicates that the barrier layer in this region occurs because of a subduction of central Pacific salty water beneath a rain-formed surface layer of freshwater [*Vialard and Delecluse,* 1998; *You,* 1998], where the latter has formed as summarized from *Anderson et al.* [1996] in section 1. We note here that sea ice formation in the Okhotsk and Bering Seas is important for the ventilation of the intermediate depths of the North Pacific [*Talley,* 1993], and this may be responsible for the barrier layer formation here. Similarly, we note that sea ice formation in the Japan Sea is associated with ventilation of the entire water column, creating the densest surface waters in the North Pacific. The shallow ILD and MLD off the coast of Alaska is because of the continental shelf extending between the North American and Eurasian continents, which is at most 100 m deep.

For latitudes below 30°N the barrier layer is in general agreement with that reported by *Sprintall and Tomczak* [1992]. Note that they used the seasonal Levitus data for their study rather than the monthly Levitus data as in the present study. A detailed comparison with their work is not possible because of the differences in climatologies, methodology, and defining ILD and MLD criteria.

The deep ILD that appears as a strong characteristic of the midlatitude North Pacific in February is markedly reduced in extent in May. This results in a barrier layer > 50 m during May that is confined to a small region off the northern continental shelf (Plate 1). This agrees with *Bathen* [1972], who found a shallow ILD in the central North Pacific between May and June. The much shallower MLD between 40° and 45°N is due to the shallow halocline that forms as a typical summer feature in response to precipitation and solar heating [*Roden,* 1977; *Webster,* 1994]. The barrier layer disappears by August and appears only slightly in November (Plate 2). The barrier layer is < 10 m over most of the North Pacific for May, August, and November and is therefore not considered significant. The barrier layer thicknesses > 10 m in the low latitudes are consistent with the findings of *Sprintall and Tomczak* [1992] and are due to a shallower halocline than thermocline, as remarked above. An interesting feature of the seasonal changes is the very shallow mixed layer for both $h_L(T)$ and $h_L(\sigma_t)$, which begins developing in May as a narrow ridge at $\approx$ 20°–25°N. By August this region has expanded to dominate almost entirely the North Pacific at midlatitudes. Maximum mixed layer depths of 75–100 m in August are limited to small regions at the equator, while north of 30°N, the MLD shallows to 25 m or less.

4.2. Turbulent Interpretation

Both a positive flux of fresh water and a positive heat flux can contribute to a positive buoyancy flux that will stabilize a surface mixed layer. When the wind is stronger and shear at the base of the mixed layer is large relative to the stratification, mixing will occur, and the surface layer will deepen until there is a balance between the mechanical mixing energy and the input of buoyancy at the surface [e.g., *Webster,* 1994]. Thus, given a simple understanding of turbulent mixing, the spatial variations in MLD mentioned above can be understood from monthly climatologies of wind stress τ, net surface heat flux Q, and freshwater fluxes (evaporation–precipitation (E–P)) such as those contained within the Comprehensive Ocean-Atmospheric Data Set (COADS) [*da Silva et al.,* 1994]. While the use of monthly means ignores the impact that short term atmospheric events such as wind bursts have in deepening the mixed layer for up to several days, they are sufficient to obtain a simple understanding of the seasonal MLD variability over the North Pacific. We also choose to ignore the influence that seasonal variations in wind stress curl, etc., have upon the MLD as they are second-order effects. Our intent here is simply to obtain an initial understanding of the MLD variability over the North Pacific and not an in-depth quantitative explanation. The amount of turbulent kinetic energy (TKE) available for mixing is well known to be directly related to surface wind stress and surface buoyancy forcing [e.g.,

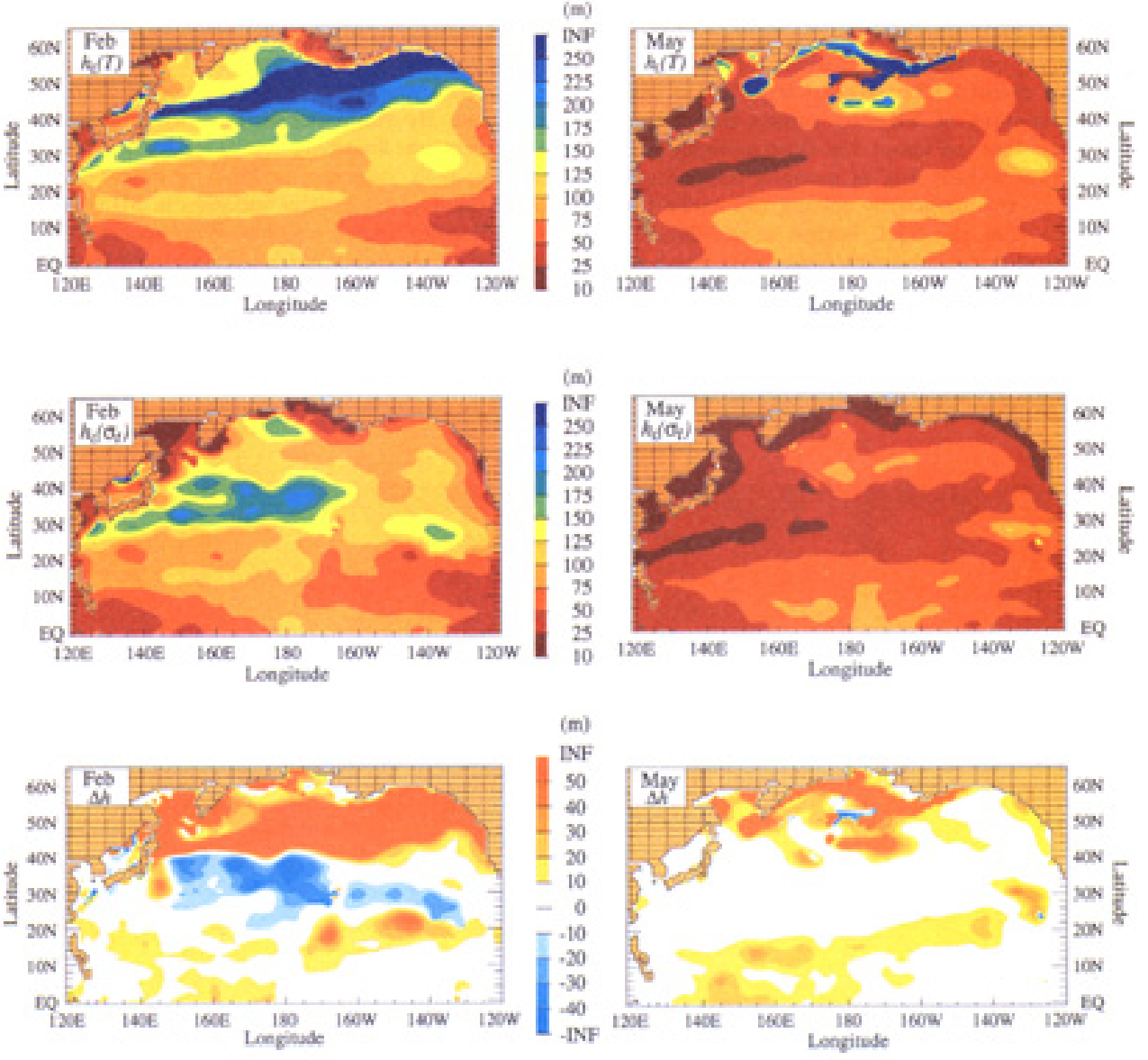

Plate 1. Layer thicknesses for the North Pacific Ocean in February and May obtained from the temperature-based criterion ILD ($h_L(T)$) and the density-based criterion MLD ($h_L(\sigma_t)$). Note that the shallowest MLD in our optimal definition is 10 m. The barrier layer (i.e., $\Delta h = h_L(T) - h_L(\sigma_t)$) is also shown for each month.

Veronis, 1973; *Gordon and Corry,* 1991]. Using the classical Kraus-Turner mixed layer model for guidance [*Kraus and Turner,* 1967; *Niiler and Kraus,* 1977], the amount of TKE (e) available when ignoring dissipation effects can be simply represented by

$$\int \frac{de}{dt}\,dz \;=\; m_3\,u_*^3 - \frac{1}{2}\frac{g\,\alpha}{\rho_s\,C_p}\,Q\,h_m. \qquad (3)$$

The first term on the right-hand side is the shear production of TKE generated by the surface wind stress τ, where $u_*^2 = \tau/\rho_a$ is the friction velocity and ρ_a is the air density. The second term is the production or damping of TKE by surface buoyancy forcing. Note that we adopt the oceanographic convention of positive heat flux as warming the ocean. The MLD (h_m) is obtained by solving (3) under the assumptions that the TKE budget is one-dimensional (the vertical fluxes are much larger than the horizontal fluxes) and stationary ($\frac{de}{dt} = 0$). All the other quantities in the equation are constants ($m_3 = 7.5$, $g = 9.81$ m s^{-2}, $\alpha = 2.5\times10^{-4}$°C^{-1}, $\rho_a = 1.21$ kg m^{-3}, $\rho_s = 1022$ kg m^{-3}, and $C_p = 3988$ J kg^{-1}°C^{-1}). From this energy balance equation one observes that the MLD deepens with increasing wind stress magnitude in order to maintain the sum of right-hand terms at zero. Note here that *Smyth et al.* [1996] and *Richardson et al.* [1999] have shown that the TKE exponentially decays with time after surface forcing is removed and that the TKE source terms continue to play a major role in changing the structure of the upper and lower parts of the mixed layer. Under conditions of heating ($Q > 0$) the MLD decreases, while for cooling ($Q < 0$), increased TKE is available for mixing. The MLD increases in the latter case by converting the TKE into potential energy via a deepening of the thermocline through entrainment. By examining the monthly wind stress and net surface heat fluxes as given by COADS (Plate 3) and knowing their influence on MLD as described above, understanding the general variation in MLD over the North Pacific Ocean is possible. While freshwater fluxes are known to be important in the equatorial Pacific [e.g., *Anderson et al.,* 1996], their effects are ignored here because their seasonal variability over the remainder of the North Pacific is much smaller than the surface heat fluxes (Figure 2), making them a second-order contribution to the surface buoyancy forcing. This small sea-

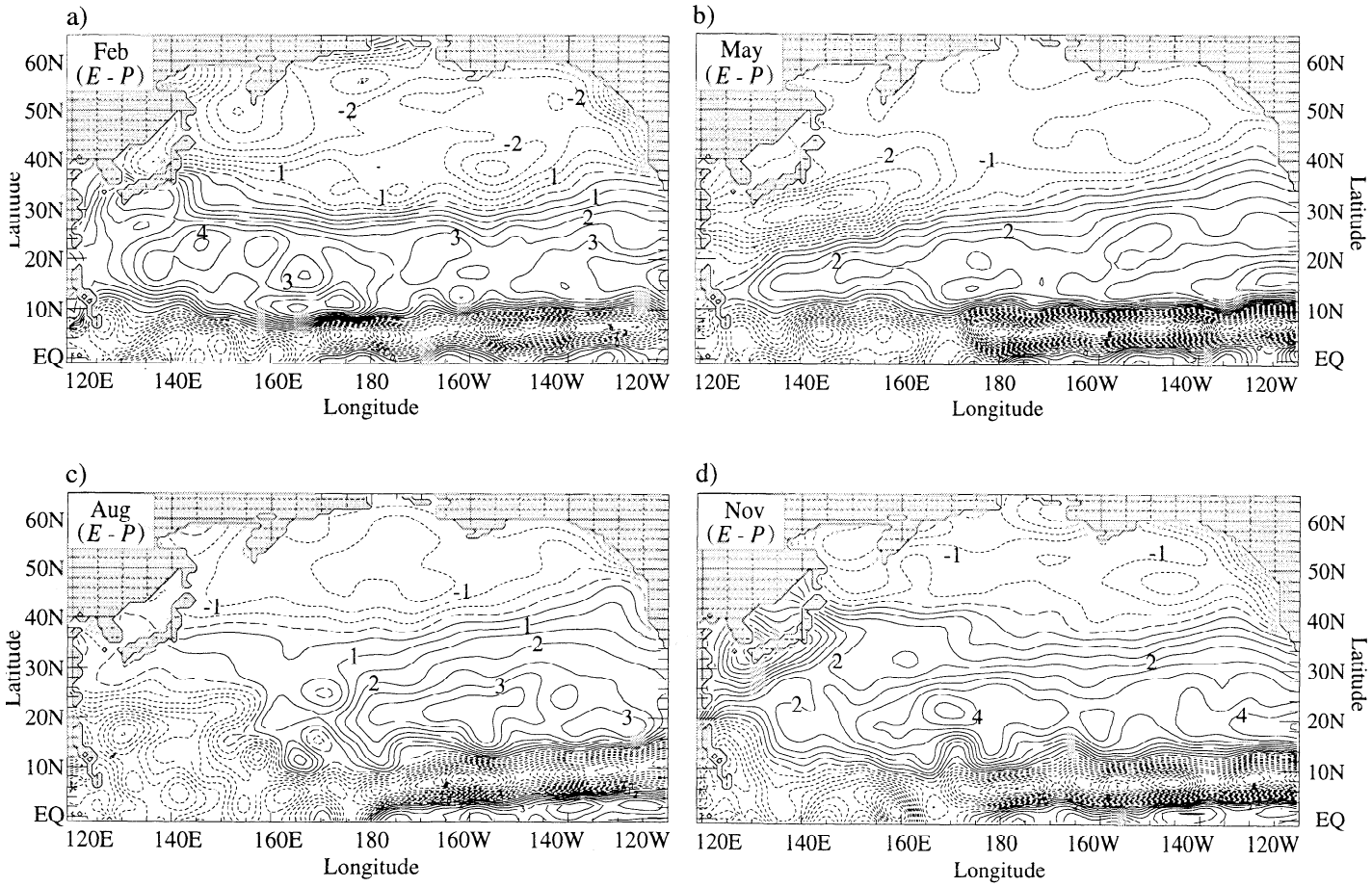

Figure 2. Monthly evaporation-precipitation (E–P) fields in mm d^{-1} for the North Pacific Ocean obtained from the Comprehensive Ocean Atmosphere Data Set (COADS) in (a) February, (b) May, (c) August, and (d) November. Dotted lines show negative values of E–P (i.e., $E < P$), solid lines show positive values of E–P (i.e., $E > P$), and the long-dashed line represents the zero contour (i.e., E=P). Note that the contour interval is 0.5 mm d^{-1}.

sonal variability in the COADS freshwater fluxes may be because they are not as well known as the surface heat fluxes.

The February MLD follows the general pattern of February wind stress magnitude (Plate 4), with the deepest MLD in the western mid-Pacific coinciding with the strongest wind stress ($\approx 0.1 - 0.2$ Pa). The mixed layer in this region is deepened further by the strong surface cooling of more than -150 W m^{-2}. The narrow shallowing of the MLD from Japan eastward to 160°E is likely due to changes in the upper ocean heat balance caused by the Kuroshio current system. This phenomena was also indicated by *Hsiung* [1985] in surface heat fluxes determined from ship measurements. She showed that a large heat loss exists in the region of the Kuroshio extension and a net heat gain exists in the tropics, which is strongest in the eastern Pacific equatorial upwelling region. Mapping the surface MLD for the North Pacific, *Reid* [1982] showed that the deepest mixed layers are found just north of the Kuroshio Extension east of 150°E in a band stretching across the Pacific that is centered south of 40°N.

A study of the local heat balance shows that horizontal advection and eddy diffusion make substantial contributions, with the heat advection warming the region west of 150°E and cooling it east of 150°E [*Qiu and Kelly,* 1993]. This can be illustrated by calculating the horizontal heat advection in the surface waters using monthly climatologies. The heat advection over a finite depth h can be approximately determined using the relation

$$\begin{aligned} Q_{\text{adv}} &= \int_{-h}^{0} \left[-\rho C_p \left(\mathbf{v} \cdot \nabla_H T\right)\right] dz \\ &= -\rho_s h C_p \left(\mathbf{v}_s \cdot \nabla_H T_s\right), \end{aligned} \tag{4}$$

where ∇_H is the horizontal gradient and ρ_s, $\mathbf{v}_s$, and T_s are the average surface density, current, and temperature, respectively. Surface currents (i.e., $\mathbf{v}$) from ship drift observations are indicative of the currents in the upper 20 m of the ocean as the Ekman component of the flow diminishes by only $\approx 25\%$ when averaged over this depth. Using a surface current climatology (A. Mariano, personal communication, 1999) and the Levitus sea temperatures at 10 m [*Levitus and Boyer,* 1994], we calculated the approximate heat advection one can expect in the upper 20 m of the ocean. This calculation yielded heat fluxes for February that varied from 75 to 200 W m^{-2} over the region 35°–45°N lying west of 150°E and from -75 to 125 W m^{-2} for the region directly east of 150°E.

The shallowing of the North Pacific mixed layer during May and August is generally consistent with the combined influence of decreased winds ($\tau < 0.1$ Pa in Plate 4) and increased surface heating ($Q > 50$ W m^{-2}) in the progression from winter to summer time conditions (Plate 3). The narrow ridge of very shallow MLD in May coincides with the region of moderate surface heating ($Q > 100$ W m^{-2}) and weak winds ($\tau < 0.025$ Pa) south of Japan. The mixed layer shallows because of decreased wind stirring and sustained moderate heating. The subsequent deepening of the mixed layer in November follows the return of stronger winds (Plate 4) and increased surface cooling ($Q < -100$ W m^{-2}). The absence of a deeper mixed layer east of Japan in November is surprising given the very strong surface cooling that occurs at this time of year. Evidence from an upper ocean heat balance study of this region indicates that the average temperature of the mixed layer decreases most rapidly in November, while the rate of mixed layer deepening is approximately the same from October through February [*Qiu and Kelly,* 1993]. This suggests that fall mixed layer deepening is more strongly controlled in this region by the presence of the seasonal thermocline that developed over the summer than by the surface cooling.

Finally, we note that thermobaric effects can influence the depth of the mixed layer. Even though the surface-based density suggests that the upper water column is stable, it can actually be unstable when cold, freshwater overlies relatively warm, salty water. This can be investigated by calculating the local density using the full equation of state [*Paluszkiewicz and Romea,* 1997]. We do not investigate this particular issue here as it only occurs in limited regions of the North Pacific for short time periods.

5. Subarctic Barrier Layer

Initial insight into the formation of the subartic barrier layer is gained by examining the observed monthly averaged temperature, salinity, and density profiles at OWS K (50°N, 145°W) as shown in Figure 3. The winter and spring pycnocline at the OWS K lies between 100 and 150 m, while the summer pycnocline is much shallower. The vertical density gradients are relatively large and shallow in the summer months compared to other seasons (see Figure 3) for reasons discussed in section 4. The ILD and MLD inferred from these profiles clearly show the effects salinity stratification has upon LD in the North Pacific. The winter ILD is deeper than the winter MLD in the eastern North Pacific because surface cooling has deepened the thermocline to below 150 m, revealing the halocline at 100–150 m. The lower-salinity surface water is due to precipations dominating over evaporation over the subpolar gyre (see Figure 2). We note here that a freshwater flux into the ocean stabilizes the surface layer and inhibits the vertical penetration of wind-driven turbulence. This reduces the entrainment of the colder and saltier subthermocline water.

To investigate how the thick barrier layer occurs over the subpolar gyre during February, we examine the vertical cross sections of Levitus temperature, salinity, and density at its widest north–south extent of the barrier layer. This occurs at ≈ 170°W longitude (Figures 4, 5, and 6). The temperature cross sections (Figure 4) reveal that the ILD in the subpolar gyre follows the devel-

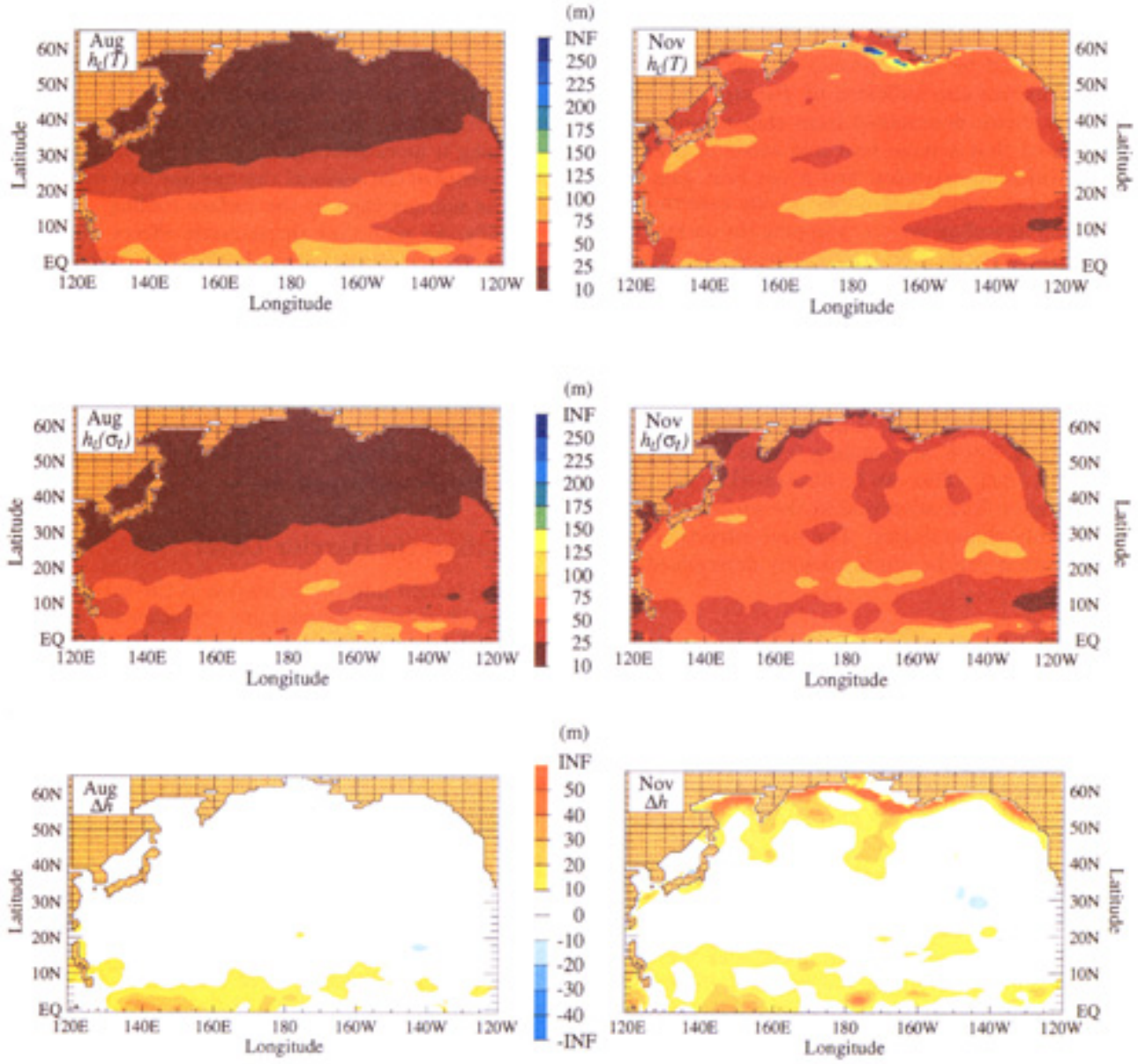

Plate 2. The same as Plate 1 but for August and November.

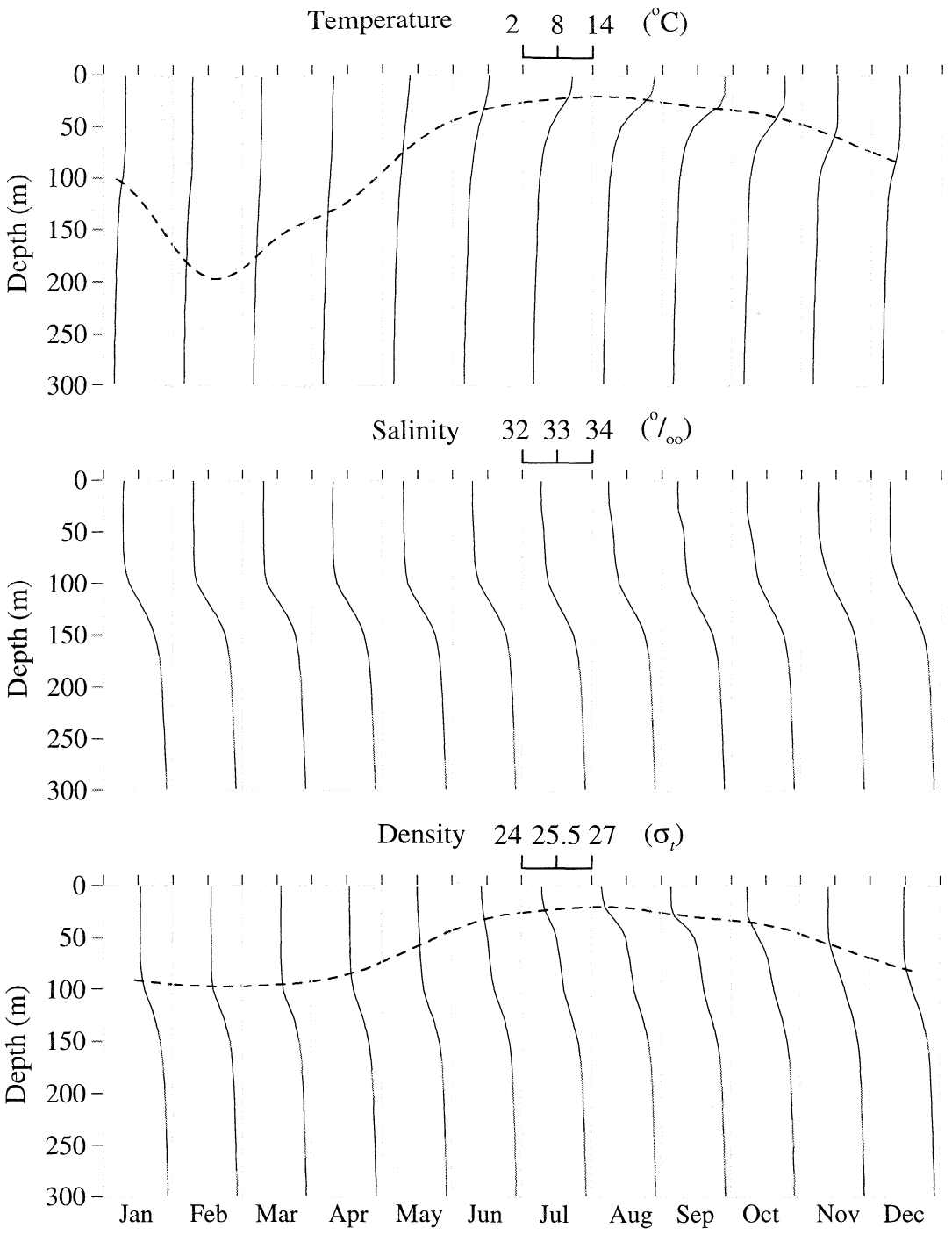

Figure 3. Monthly averaged temperature, salinity, and density profiles at OWS K (50°N,145°W) from January to December. Monthly data used are constructed from 1959 to 1990. Overlayed as a dashed line on the isotherms (isopycnics) is the ILD (MLD) for a ΔT value of 0.8°C. Note here that the x axis scaling is the same for each of the individual monthly temperature, salinity, and density profiles.

opment of the seasonal thermocline during the surface heating of May and August and its subsequent erosion under the surface cooling of November and February. Note that the deep ILD in February occurs during a time of weak wind stress ($\tau < 0.075$ Pa) as seen from Plate 3, suggesting that it is due to wind stirring, although a contribution from winter storms is not ruled out. The narrowing of the deep ILD plume region in May is noted to coincide with the return of surface heating and modest wind stress of $0.05 < \tau < 0.10$ Pa.

The density cross sections (Figure 5) follow the seasonal changes in temperature cross sections at low latitudes and the seasonal thermocline variations from shallower to deeper at midlatitudes from winter through to

autumn. This is clear when comparing the ILD and MLD, which exhibit the same spatial dependence at low latitudes to $\approx 40°$N in all seasons and at subpolar latitudes during summer and autumn. This similarity between the major seasonal changes in the density and temperature indicates that density stratification is most strongly influenced by the changes in temperature in these regions during these months. Given that the thermocline follows the seasonal cycle in surface heat fluxes (see Plate 3), one infers that the MLD coincides with the ILD because of the development of the seasonal thermocline because of surface heating. The much shallower MLD than ILD at subpolar latitudes during winter and spring is due to salinity stratifications becom-

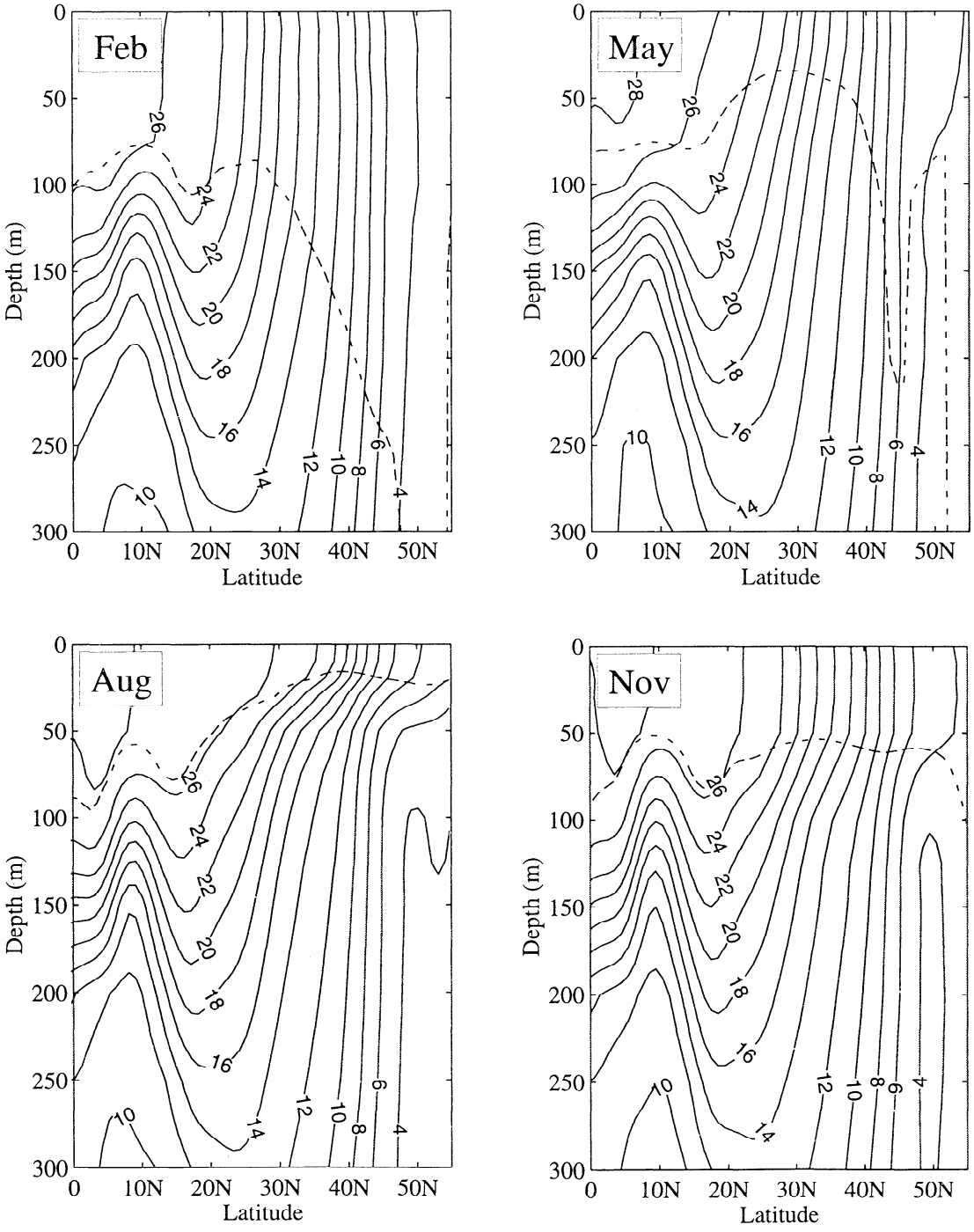

Figure 4. Vertical cross sections of temperature (in degrees Celsius) along 170°W in the North Pacific Ocean for February, May, August, and November. Overlayed as a dashed line on the isotherms is the ILD ($h_L(T)$) for each season for a ΔT value of 0.8°C. The contour interval is 2°C.

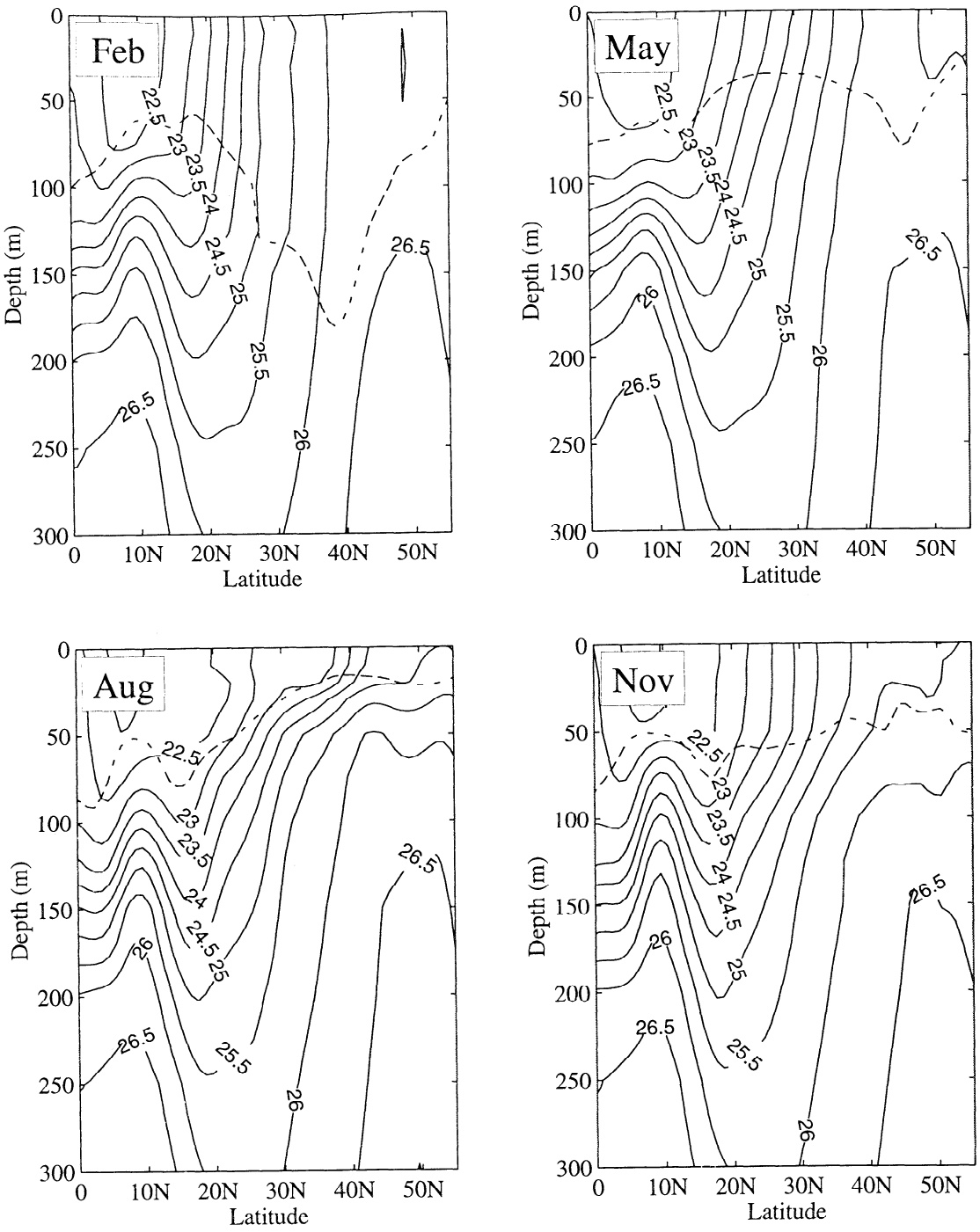

Figure 5. Vertical cross sections of density (in σ_t) along 170°W in the North Pacific Ocean for February, May, August, and November. Overlayed as a dashed line on the isopycnals is the MLD ($h_L(\sigma_t)$) for each season for a ΔT value of 0.8°C. The contour interval is $0.5\,\sigma_t$. The unstable density stratification near the surface in the cross sections are consequences of the temperature and salinity inversions inherent to the Levitus data.

ing important (Figure 6). The salinity cross sections show that salinity has small seasonal variability with the largest changes occurring at 0–10°N. During winter and spring the strong surface cooling (Plate 3) has eroded away the seasonal thermocline to produce a deep isothermal layer (Figure 4). This allows an MLD influenced by the halocline (see Figure 6), which lies above the deeper main thermocline (see Figure 4). This halocline is what is limiting the MLD to depths generally < 125 m north of 40°N during winter and to a lesser extent during spring.

The appearance of this subarctic barrier layer in winter because of surface cooling becomes further evident when examining properties from the annual Levitus cli-

matology. The ILD and MLD obtained from the annual Levitus temperature and density, respectively, provide no indication of a thick barrier layer in the subarctic (Figure 7). The signal of greater deepening of the thermocline relative to the pycnocline at 40°–50°N in winter is lost in the annual average. However, the annual salinity cross section is quite similar to those for each of the four seasons because of the low seasonal variability in salinity.

In summary, the cyclonic subpolar gyre lies north of the subarctic front, which spans the North Pacific Ocean between between 40° and 45°N [*Thomson et al.*, 1998]. The prominent wintertime barrier layer (ILD > MLD) coincides with the subpolar gyre and covers most of it (see Plate 1). This barrier layer forms when the seasonal thermocline erodes, uncovering a permanent halocline at 100–150 m depth (see Figures 3 and 5) and a permanent isothermal layer, which

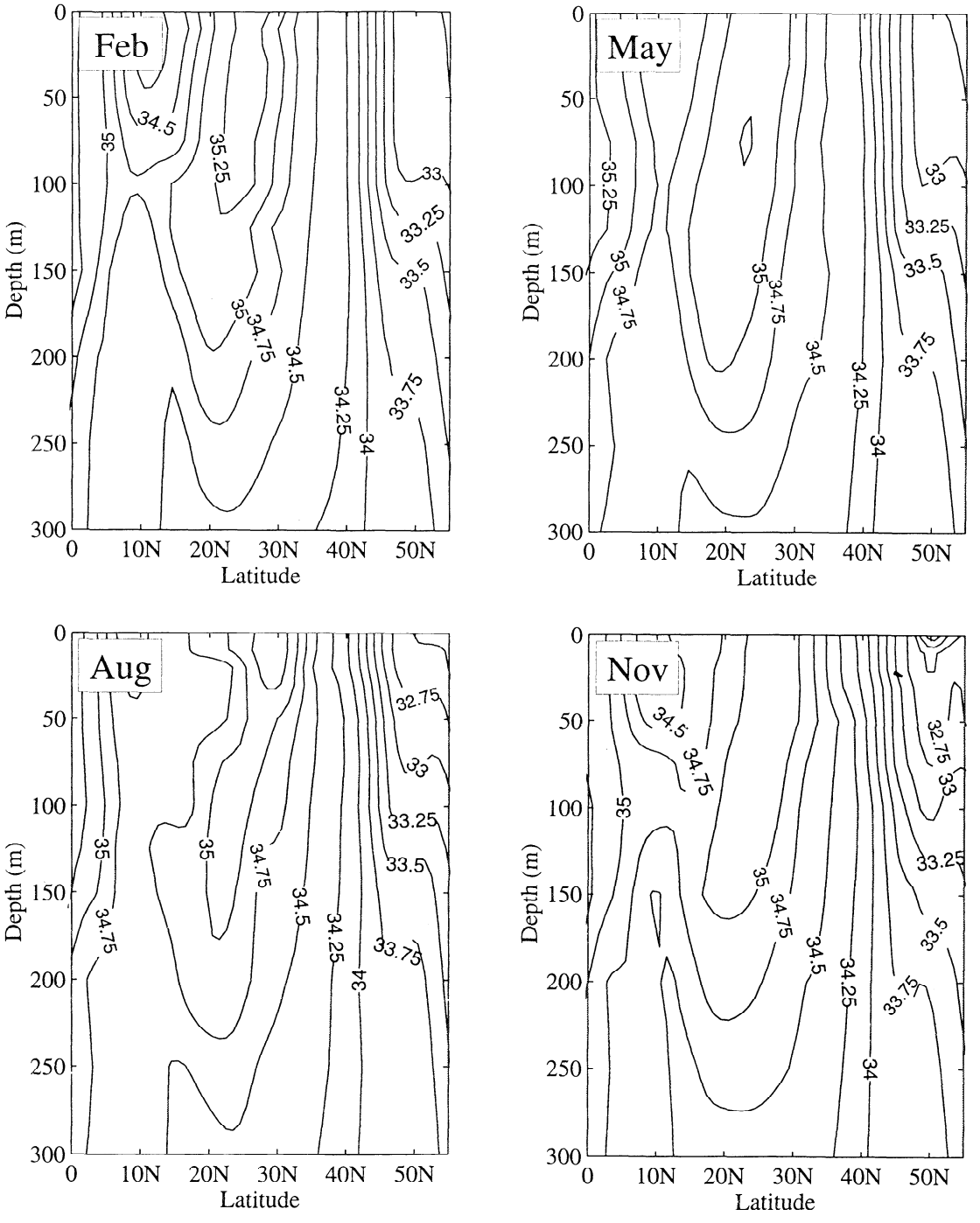

Figure 6. Vertical cross sections of salinity (parts per thousand) along 170°W in the North Pacific Ocean for February, May, August, and November. The contour interval is 0.25 per thousand.

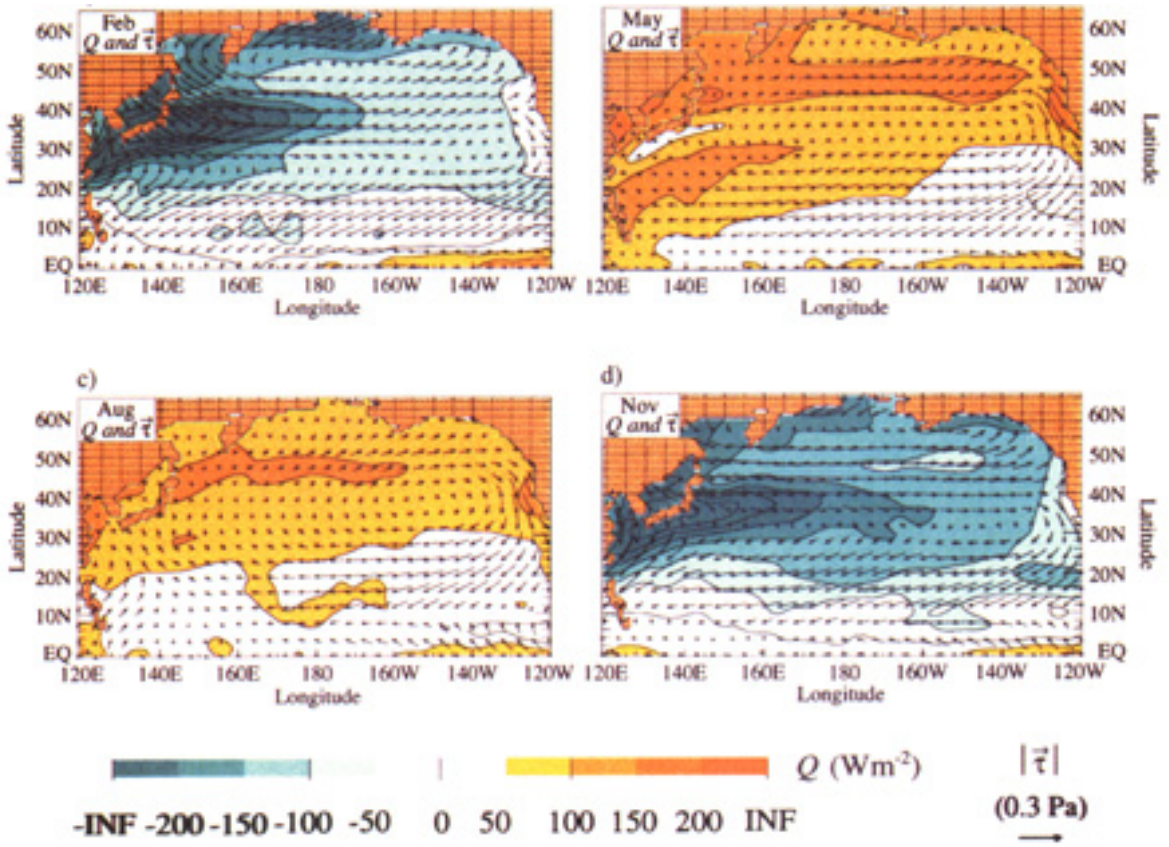

Plate 3. Monthly wind stress τ in Pascal denoted as Pa (Pa = N m^{-2}) and net surface heat flux Q in Watts per meter square (W m^{-2}) for the North Pacific Ocean obtained from the Comprehensive Ocean Atmosphere Data Set (COADS) in (a) February, (b) May, (c) August, and (d) November. The heat flux contour interval is 50 W m^{-2}, and the magnitude of the wind stress reference vector (τ) is 0.3 N m^{-2}.

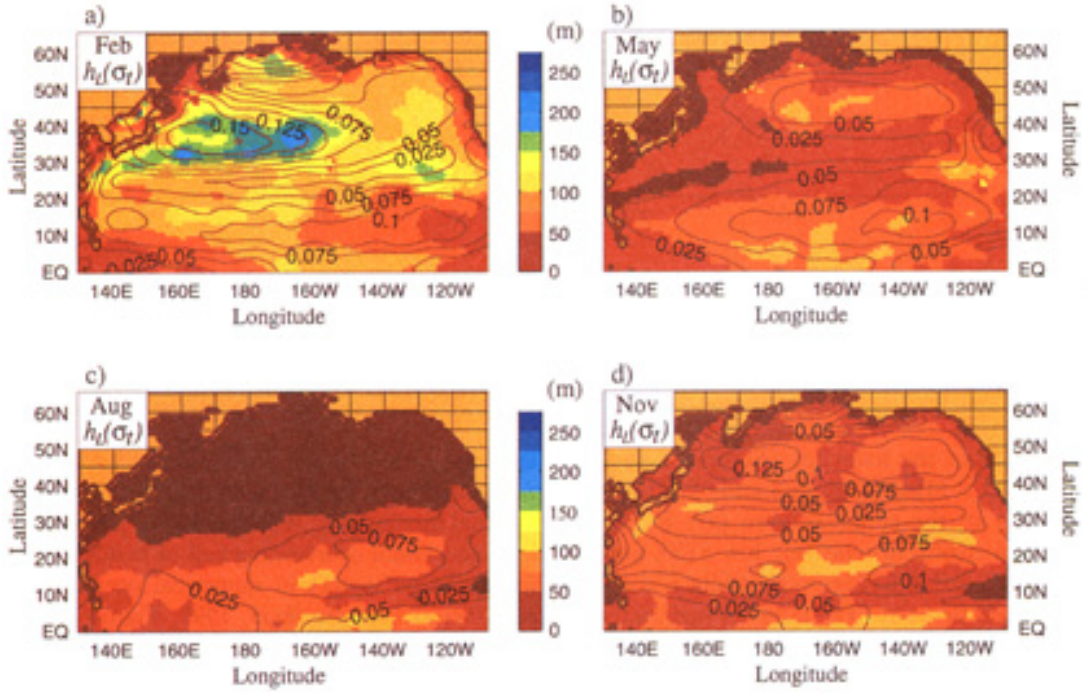

Plate 4. The monthly MLD ($h_L(\sigma_t)$) in meters and COADS wind stress magnitude (τ) in Pascal for the North Pacific Ocean in (a) February, (b) May, (c) August, and (d) November. The MLD contour interval is 25 m, and the wind stress contour interval is 0.025 Pa.

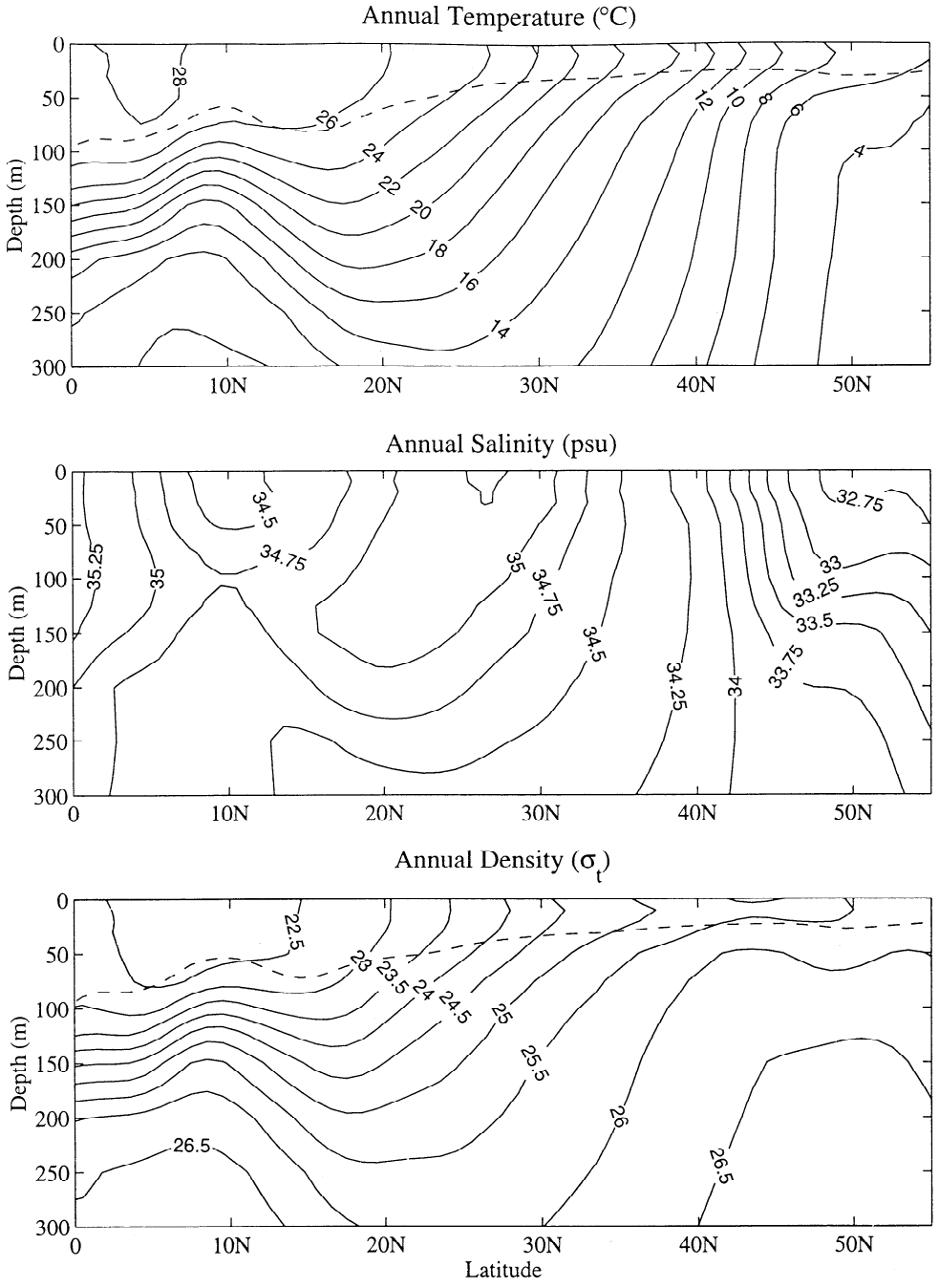

Figure 7. Vertical cross sections of annual mean temperature (in degrees Celsius), salinity (per thousand), and density (in σ_t) along 170°W in the North Pacific. The unstable density stratification near the surface is a consequences of the temperature and salinity inversions inherent to the Levitus data.

extends deeper than the halocline (Figures 3 and 4), thus allowing ILD > MLD (Figures 3 and 6). The halocline is confined to the subpolar gyre (see Figure 6) because this is a region of relatively low SSTs and an annual mean of $E - P < 0$ (Figure 8), while $E - P > 0$ south of the subarctic front. The input of surface freshwater ($E - P < 0$) allows the formation of a relatively fresh surface layer in the subpolar gyre. The halocline must be maintained from below by net upward vertical motion. Positive mean wind stress curl over the subpolar gyre provides a mechanism for this by forcing Ekman suction, isopycnal doming, and slow upward diapycnal mixing [e.g, *Webster,* 1994]. This drives a shallow meridional overturning cell of ≈ 4 Sv in the upper few hundred meters in numerical ocean models [e.g., see *Shriver and Hurlburt,* 1997, Figure 3a]. The net northward subsurface transport of this cell would advect higher-salinity northward as shown in Figures 5 and 7, which again is critical to the maintenance of the halocline.

6. Conclusions

Seasonal changes in the ocean can result in deeper thermoclines than pycnoclines and can produce a region from the bottom of the pycnocline to the top of the thermocline known as a barrier layer. Using isothermal layer depths (ILD) and mixed layer depths (MLD) from the Naval Research Laboratory Ocean Mixed Layer Depth (NMLD) climatology that were constructed from Levitus data, we have shown that barrier layers of up to 80 m or more can occur in the northeast Pacific during the nonsummer seasons. The layer depths obtained from the OWS climatologies have been used to verify our results. In general, the ILD and MLD inferred from the monthly NMLD climatology reveals that this barrier layer generally coincides with the subpolar gyre and has a thickness > 50 m in winter. At lower latitudes close to the equator the barrier layer has an absolute thickness that averages to < 20 m.

The formation of the thick subarctic barrier layer in winter occurs because of moderate seasonal cooling that erodes the seasonal thermocline, revealing a deeper isothermal layer beneath. The surface cooling deepens the thermocline sufficiently such that the halocline, which has been shallowed in the subpolar gyre region because of surface fresh water, becomes important in defining the mixed layer. Positive wind stress curl over the subpolar gyre provides a mechanism for maintaining the halocline at the intermediate depths of 100–150 m. This thereby limits the MLD to less than the ILD. The retreat of the barrier layer to higher latitudes in spring and its subsequent disappearance in summer and fall follows the development of the seasonal thermocline with the annual cycle of surface heating and, to a much lesser extent, the seasonal halocline with the freshwater fluxes. Temperature becomes the controlling influence for the density in these nonwinter seasons and results in a pycnocline at the same depth as the seasonal thermocline. The occurrence of such thick barrier layers emphasizes the importance of using density when defining MLD rather than ILD. Only during summer can the ILD be used as a reliable substitute for the MLD. Of course, caution must be used in the equatorial regions given evidence that climatological estimates yield barrier layers that are 20 m too thick.

We have shown that the general features of the MLD variability can be explained by examining monthly climatologies of wind stress magnitude and heat flux with guidance from the Kraus-Turner model. Departures from such a simple interpretation of MLD variability using surface forcing fields occur in the region of Kuroshio where heat advection plays a significant role. Evidence suggests that the fall mixed layer deepening in the Kuroshio region is more controlled by erosion of the seasonal thermocline by surface cooling outside regions of strong advection. We note that formation of the subarctic barrier layer is a seasonal phenomenon produced by local processes associated with heat flux,

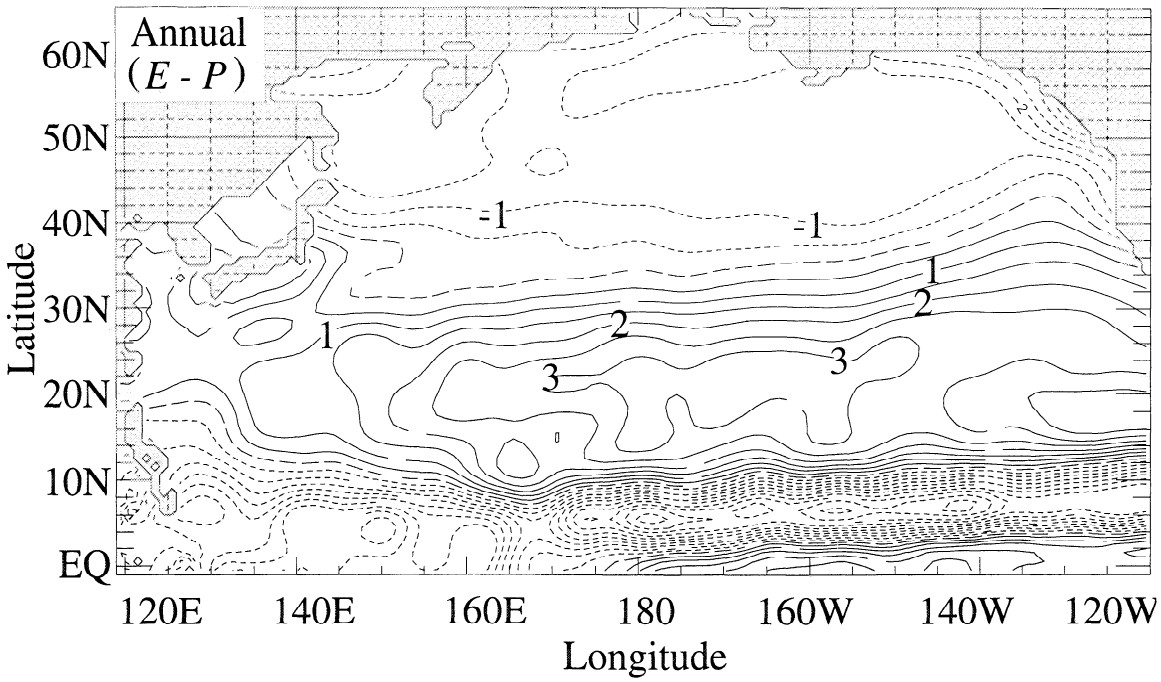

Figure 8. Annual mean of evaporation–precipitation (E–P) fields in mm d^{-1} for the North Pacific Ocean obtained from the Comprehensive Ocean Atmosphere Data Set (COADS). Dotted lines show negative values of E–P (i.e., $E < P$), solid lines show positive values of E–P (i.e., $E > P$), and the long-dashed line represents the zero contour (i.e., E=P). Note that the contour interval is 0.5 mm d^{-1}.

rather than high precipitation and/or westward subduction of higher–salinity water as in the western equatorial Pacific. For these reasons, calling it a barrier layer is somewhat of a misnomer. However, we refer to it as such to be consistent with the nomenclature in the scientific literature.

Finally, this paper has presented the first application of the NMLD climatology that was constructed using the optimal MLD definition determined by *Kara et al.* [this issue]. Our experience in using the NMLD climatology for validation of the Naval Research Laboratory Layered Ocean Model has shown that it can serve as an invaluable data set for identifying deficiencies in an ocean general circulation model with an embedded mixed layer. The NMLD climatology is available to other researchers.

Acknowledgments. We would like to thank A. J. Wallcraft of the Naval Research Laboratory (NRL), Stennis Space Center, for his discussions. Additional thanks go to A. Mariano of the Rosenstiel School of Marine & Atmospheric Science, University of Miami, for providing the surface current climatology. Finally thanks also go to Amy Summers for her work on the color figures. Constructive criticism made by reviewers is greatly appreciated. This work was funded by the Office of Naval Research (ONR) and is a contribution of the Basin-Scale Prediction System project under program element 602435N and the Dynamics of Coupled Air-Ocean Models Study under program element 61153N. Sverdrup Technology, Inc., is funded under subcontract from the NRL. This is contribution NRL/JA/7323-99-0028 and has been approved for public release.

References

Anderson, S. P., R. A. Weller, and R. B. Lukas, Surface buoyancy forcing and the mixed layer of the western Pacific warm pool: Observations and 1D model results, *J. Clim.*, *9*, 3056–3085, 1996.

Ando, K., and M. J. McPhaden, Variability of surface layer hydrography in the tropical Pacific Ocean, *J. Geophys. Res.*, *102*, 23,063–23,078, 1997.

Bathen, K. H., On the seasonal changes in the depth of the mixed layer in the North Pacific Ocean, *J. Geophys. Res.*, *77*, 7138–7150, 1972.

Chen, D., A. J. Busalacchi, and L. M. Rothstein, The roles of vertical mixing, solar radiation, and wind stress in a model simulation of the sea surface temperature seasonal cycle in the tropical Pacific Ocean, *J. Geophys. Res.*, *99*, 20,345–20,359, 1994.

da Silva, A. M., C. C. Young, and S. Levitus, *Atlas of Surface Marine Data 1994, vol. 1, Algorithms and Proccdurcs*, 83 pp., U.S. Govt. Print. Off., Washington, D.C., 1994.

Dinniman, M. S., and M. M. Rienecker, Frontogenesis in the North Pacific oceanic frontal zones, *J. Phys. Oceanogr.*, *29*, 537–559, 1999.

Enfield, D. B., Zonal and seasonal variability of the equatorial Pacific heat balance, *J. Phys. Oceanogr.*, *16*, 1038–1054, 1986.

Gent, P. R., The heat budget of the TOGA–COARE domain in an ocean model, *J. Geophys. Res.*, *96*, 3323–3330, 1991.

Godfrey, J. S., and E. Lindstrom, The heat budget of the equatorial western Pacific surface mixed layer, *J. Geophys. Res.*, *94*, 8007–8017, 1989.

Gordon, C., and R. A. Corry, A model simulation of the seasonal cycle in the tropical Pacific Ocean using climatological and modeled surface forcing, *J. Geophys. Res.*, *96*, 847–864, 1991.

Hsiung, J., Estimates of global oceanic meridional heat transport, *J. Phys. Oceanogr.*, *15*, 1405–1413, 1985.

Hurlburt, H. E., A. J. Wallcraft, W. Schmitz Jr., P. J. Hogan, and E. J. Metzger, Dynamics of the Kuroshio/-Oyashio current system using eddy-resolving models of the North Pacific Ocean, *J. Geophys. Res.*, *101*, 941–976, 1996.

Kara, A. B., P. A. Rochford, and H. E. Hurlburt, An optimal definition for ocean mixed layer depth, *J. Geophys. Res.*, this issue.

Kraus, E. B., and J. S. Turner, A one-dimensional model of the seasonal thermocline, II, The general theory and its consequences, *Tellus*, *19*, 98–105, 1967.

Lamb, P. J., On the mixed layer climatology of the north and tropical Atlantic, *Tellus, Ser. A*, *36*, 292–305, 1984.

Levitus, S., R. Burgett, and T. P. Boyer, *World Ocean Atlas 1994*, vol. 3, *Salinity, NOAA Atlas NESDIS 3*, 99 pp., U.S. Govt. Print. Off., Washington, D.C., 1994.

Levitus, S., and T. P. Boyer, *World Ocean Atlas 1994*, vol. 4, *Temperature, NOAA Atlas NESDIS 4*, 117 pp., U.S. Govt. Print. Off., Washington, D.C., 1994.

Lindstrom, E., R. Lukas, R. Fine, E. Firing, S. Godfrey, G. Meyers, and M. Tsuchiya, The western Equatorial Pacific Ocean Circulation Study, *Nature*, *330*, 533–537, 1987.

Lukas, R., and E. Lindstrom, The mixed layer of the western equatorial Pacific Ocean, *J. Geophys. Res.*, *96*, 3343–3357, 1991.

Meyers, G., J.-R. Donguy, and R. K. Reed, Evaporative cooling of the western equatorial Pacific Ocean by anomalous winds, *Nature*, *323*, 523–526, 1986.

Miller, J. R., The salinity effect in a mixed layer ocean model, *J. Phys. Oceanogr.*, *6*, 29–35, 1976.

Monterey, G., and S. Levitus, *Seasonal Variability of Mixed Layer Depth for the World Ocean, NOAA Atlas NESDIS 14*, 100 pp., U.S. Govt. Print. Off., Washington, D.C., 1997.

Niiler, P. P., and E. B. Kraus, One-dimensional models of the upper ocean, in *Modeling and Prediction of the Upper Layers of the Ocean*, edited by E. B. Kraus, pp. 143–172, Pergamon, Tarrytown, N.Y., 1977.

Niiler, P. P., and J. Stevenson, The heat budget of tropical ocean warm-water pools, *J. Mar. Res.*, *40*, 465–480, 1982.

Obata, A., J. Ishizaka, and M. Endoh, Global verification of critical depth theory for phytoplankton bloom with climatological in situ temperature and satellite ocean color data, *J. Geophys. Res.*, *101*, 20,657–20,667, 1996.

Ohlmann, J. C., D. A. Siegel, and C. Gautier, Ocean mixed layer radiant heating and solar penetration: A global analysis, *J. Climate*, *9*, 2265–2280, 1996.

Paluszkiewicz, T., and R. D. Romea, A one-dimensional model for the parameterization of deep convection in the ocean, *Dyn. Atmos. Oceans*, *26*, 95–130, 1997.

Piola, A. R., and A. Gordon, Pacific and Indian Ocean upper layer salinity budget, *J. Phys. Oceanogr.*, *14*, 747–753, 1984.

Price, J. F., R. A. Weller, and R. Pinkel, Diurnal cycling: Observations and models of the upper ocean response to diurnal heating, cooling, and wind mixing, *J. Geophys. Res.*, *91*, 8411–8427, 1986.

Qiu, B., and T. M. Joyce, Interannual variability in the mid- and low-latitude western North Pacific, *J. Phys. Oceanogr.*, *22*, 1062–1079, 1995.

Qui, B., and K. A. Kelly, Upper-ocean heat balance in the Kuroshio Extension region, *J. Phys. Oceanogr.*, *23*, 2027–2041, 1993.

Rao, R. R., R. L. Molinari, and J. F. Festa, Evolution of the

climatological near-surface thermal structure of the tropical Indian Ocean, 1, Description of mean monthly mixed layer depth, and sea surface temperature, surface current, and surface meteorological fields, *J. Geophys. Res., 94*, 10,801–10,815, 1989.

Reid, J. L., Evidence of an effect of heat flux from the east Pacific rise upon on characteristics of the mid-depth waters, *Geophys. Res. Lett., 9*, 381–384, 1982.

Richardson, R. A., G. G. Sutyrin, D. Hebert, and L. M. Rothstein, Universality of the modeled small-scale response of the upper tropical ocean to squall wind forcing, *J. Phys. Oceanogr., 29*, 519–529, 1999.

Roden, G. I., Oceanic subarctic fronts of the central Pacific: Structure of and response to atmospheric forcing, *J. Phys. Oceanogr., 7*, 761–778, 1977.

Roden, G. I., The depth variability of meridional gradients of temperature, salinity and sound velocity in the western North Pacific, *J. Phys. Oceanogr., 9*, 756–767, 1979.

Roden, G. I., On the variability of surface temperature fronts in the western Pacific, as detected by satellite, *J. Geophys. Res., 85*, 2704–2710, 1980.

Shriver, J. F., and H. E. Hurlburt, The contribution of the global thermohaline circulation to the Pacific to Indian Ocean Throughflow via Indonesia, *J. Geophys. Res., 102*, 5491–5511, 1997.

Smyth, W. D., P. O. Zavialov, and J. N. Moum, Decay of turbulence in the upper ocean following sudden isolation from surface forcing, *J. Phys. Oceanogr., 27*, 810–822, 1996.

Sprintall, J., and D. Roemmich, Characterizing the structure of the surface layer in the Pacific Ocean, *J. Geophys. Res., 104*, 23,297–23,311, 1999.

Sprintall, J., and M. Tomczak, Evidence of the barrier layer in the surface layer of tropics, *J. Geophys. Res., 97*, 7305–7316, 1992.

Swenson, M. S., and D. V. Hansen, Tropical Pacific Ocean mixed layer heat budget: The Pacific cold tongue, *J. Phys. Oceanogr., 29*, 69–81, 1999.

Talley, L. D., Distribution and formation of North Pacific intermediate water, *J. Phys. Oceanogr., 23*, 517–537, 1993.

Teague, W. J., M. J. Carron, and P. J. Hogan, A comparison between the generalized digital environmental model and Levitus climatologies, *J. Geophys. Res., 95*, 7167–7183, 1990.

Thomson, R. E., P. H. Leblond, and, A. B. Rabinovich, Satellite-tracked drifter measurement of inertial and semidiurnal currents in the northeast Pacific, *J. Geophys. Res., 103*, 1039–1052, 1998.

Tsuchiya, M., On the Pacific upper-water circulation, *J. Mar. Res., 40*, suppl., 777–799, 1982.

Veronis, G., Model of world ocean circulation, part III, Thermally and wind-driven. *J. Mar. Res., 36*, 1–44, 1973.

Vialard, J., and P. Delecluse, An OGCM study for the TOGA decade, part II, Barrier-layer formation and variability, *J. Phys. Oceanogr., 28*, 1089–1106, 1998.

Webster, P. J., The role of hydrological processes in ocean-atmosphere interactions, *Rev. Geophys., 32*, 427–476, 1994.

You, Y., Salinity variability and its role in the barrier layer formation during TOGA–COARE, *J. Phys. Oceanogr., 25*, 2778–2807, 1995.

You, Y., Rain–formed barrier layer of the western equatorial Pacific warm pool: A case study, *J. Geophys. Res., 103*, 5361–5378, 1998.

Yuan, X., and L. D. Talley, Shallow salinity minima in the North Pacific, *J. Phys. Oceanogr., 22*, 1302–1316, 1992.

H. E. Hurlburt, and P. A. Rochford, Oceanography Division, Naval Research Laboratory, Stennis Space Center, MS 39529. (hurlburt@nrlssc.navy.mil; rochford@nrlssc.navy.mil.)

A. B. Kara, Advanced Systems Group, Sverdrup Technology, Inc., Stennis Space Center, MS 39529. (kara@nrlssc.navy.mil)

(Received July 19, 1999; revised March 1, 2000;
accepted March 17, 2000.)